Journal of Ultrafine Grained and Nanostructured Materials
https://jufgnsm.ut.ac.ir
Vol. 51, No.2, December 2018, pp. 193-200
Print ISSN: 2423-6845 Online ISSN: 2423-6837
DOI: 10.22059/JUFGNSM.2018.02.12

Fabrication of functionally graded Ni-Al_2O_3 nanocomposite coating and evaluation of its properties

Zahra Noroozi[1], Masoud Rajabi[1], Behrooz Bostani *,[2]

[1]Department of Metallurgy and Materials Engineering, Faculty of Technology and Engineering, Imam Khomeini International University (IKIU) Qazvin, Iran.

[2]Department of Chemical and Materials Engineering, Buein Zahra Technical University, Buein zahra, Qazvin, Iran.

Recieved: 26 May 2018; Accepted: 5 September 2018

** Corresponding author email: bostani.behruz@gmail.com*

ABSTRACT

In this study, functionally graded Ni-Al_2O_3 composite coating (FGN-A) has been produced from nickel Watt's bath containing different concentrations of Al_2O_3 particles. Therefore, different composite coatings were electroplated in the same bath with different particles concentrations. It's to find the optimum concentration of the particles that the maximum content with uniform distribution of Al_2O_3 particles in the coating can be achieved. So, Al_2O_3 concentration was continuously increased in the electroplating bath. The composite coatings were characterized by SEM and EDS. Structure and phase composition were identified by XRD analysis. Microhardness of the coatings was evaluated by using Vickers Instrument. Three-point bend test was carried out to compare the adhesion strength of the coatings and dry sliding wear tests were performed using a pin-on-disk wear apparatus. Study on the results shows that FGN-A by Al_2O_3 gradient distribution in cross-section is coated successfully. By increasing Al_2O_3 particles content in Ni matrix, microhardness grows from interface towards the surface of the coating. The result of bending test shows that the functionally graded composite coating has excellent adhesion to substrate compared with the uniformly distributed Ni-Al_2O_3 (UN-A) on the same substrate. This has been attributed to lower mechanical mismatch between coating and substrate in functionally graded composite coating compared with uniformly distributed one. The results of wear resistance measurements test reveals that wear resistances of functionally graded Ni-Al_2O_3 is higher than that of ordinary distributed composite coating.

Keywords: *Functionally composite coating; Co-electrodeposition; Microhardness; Adhesion; Wear resistance.*

1. Introduction

Metal matrix composite (MMC) coatings have been studied for decades and successfully applied in the automotive and aerospace industry due to their excellent tribological properties, good corrosion and wear resistance, higher microhardness and longer fatigue life as compared to metallic coatings. Electroplated MMC coatings consist of oxide or carbide particles such as TiO_2, Al_2O_3, La_2O_3, SiC, co-electrodeposited in a metallic matrix such as nickel. Some techniques like chemical vapor deposition, physical vapor deposition and thermal spray are

used to produce metal matrix composite coatings. Among this techniques co-electrodeposition is the low cost and low temperature one to produce these coatings, that lots of studies have done based on this technique [1-9].

Ceramic particles are inert and hard, and are used more than other particles in co-electrodeposition, but these particles reduce the adhesion between coating and substrate [10–12]. As a result their wear resistance significantly reduces, so delamination and spallation of the coatings increase. On the other hand, co-electrodeposition of particles in the metallic matrix results in reduction in matrix's grain size, so mechanical mismatch between brittle coating and ductile substrate is increased that causes an increase in stress concentration and weak interface [13, 14].

To solve this problem, gradient composite coatings are produced recently, that have got lower mechanical mismatch. Changes in lots of parameters like amount of powder in watts bath, current density, and etc are used to produce such coatings [15–19].

The aim of this study is a FGN-A which has perfect hardness in the surface and the best adhesion to the substrate. So, to have gradient Al_2O_3 particles in the coating, the amount of particles concentration in the bath has been changed continuously during the co-electrodepositing. The wear resistance and adhesion of this gradient coating have been compared with those of the uniformly distributed composite coating.

2. Materials and Methods

By using Watt's bath Pure Ni, and Ni-Al_2O_3 composite coatings were electroplated. Details of the bath composition, electroplating procedure and preparation of samples have been shown in table 1. 20 g/l alumina powder (<5mm) was dispersed in the electroplating bath to produce UN-A composite coating, but in the case of graded Ni-Al_2O_3 composite coating, Al_2O_3 content were continuously increased from 0 to 20 g/l with a constant stirring rate of 200 rpm.

Coatings surface morphologies were examined employing SEM (Cam Scan™ model MV2300 SEM operated at 30 kV). Coating's chemical composition was recognized by using an EDS system (Oxford™). Five measurement trials were done and the results were averaged for each sample. Microhardness assessment of the coating was performed using Vickers instrument (LECO™ AT-101) by applying 25 g load in 10 s. Four microhardness measurements were conducted and results were then averaged. To compare the adhesion strength of FGN-A composite coating with that of UN-A composite coating on the st37 steel the three-point bend test was used. The dimension of samples was 1.5 cm×5 cm and the interval between two supporting points was 3.5 cm. Coating's wear resistance was studied by pin-on-disk method at room temperature. Applied force from pin to coating in 8 N, and radius of 5 mm for 50 m sliding, also before doing each experiment, all sample surfaces were cleaned and washed with acetone and dried, and for measuring the weight

Table 1- Composition of bath and conditions of electroplating procedure

Materials and variables	Amount
Nickel sulphate	250 (g/l)
Nickel chloride	40 (g/l)
Boric acid	45 (g/l)
Sodium citrate	50 (g/l)
Dodecyl sodium sulphate	0.1 (g/l)
Current density	3 (A/dm^2)
Temperature	54±1°C
Plating time	60 min
Stirring rate	200 rpm
pH	3.8-4

loss of the coatings and their pins before and after the experiment, digital balance with accuracy of 0.1 mg was used. The XRD spectra of the samples were recorded, and (111) peak broadening of fcc nickel was used to determine the average crystallite size of the nickel matrix. Equation 1 (Scherrer equation) was used to calculate the crystallite sizes.

$$L = \frac{\lambda}{\beta \times \cos\theta} \quad \text{(eq. 1)}$$

Where L is the crystallite size, λ is the X-ray wavelength, β the effective line broadening and θ the Bragg angle. β was obtained using the full width of the line measured at half maximum which was then corrected for instrumental broadening. For this correction, LaB_6 standard reference material (SRM 660a) was used.

3. Results and discussion

Weight percent changes of deposited alumina particles in different concentrations of Al_2O_3 powder in watts bath are shown in Fig. 1. Weight percent of alumina in the coating is increased until powder concentration in electrolyte reaches 20 g/l, after passing the optimum amount of powder in electrolyte, the increase in particles concentration leads to the reduction in deposited alumina in the coating. By an increase in Al_2O_3 concentration up to 20 g/l, alumina particles movement towards the specimen is more probable which leads to more deposited particles in the coating. On the other hand, adding more powder to electrolyte causes more contact between particles and leads to an agglomeration of powders, so a decrease in deposited particles happens to the coating. In powder concentrations which are more than

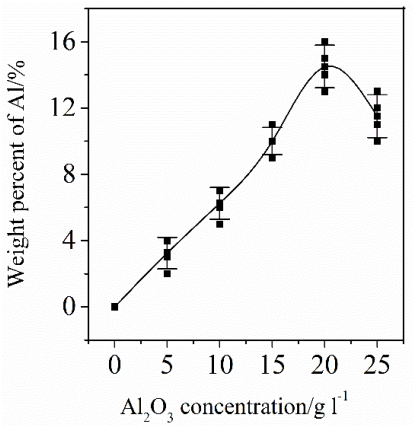

Fig. 1- Weight percent of Al in the coatings versus concentration of particles in the bath.

20 g/l agglomeration overcomes the probability of particles movement towards the surface of the coating, and increasing the concentration of particles in the bath causes a decrease in second phase particles depositing in the coating.

The SEM images of coated specimens with concentrations 0, 15, 20 and 25 g/l Al_2O_3 in the electrolyte show that maximum particles amount and the best distribution of Al_2O_3 particles in the coating is obtained from the watts bath with 20 g/l particles concentration (Fig. 2). These results show that the sample electroplated in the watts bath with 20 g/l Al_2O_3 has the most of particles and the best distribution of particles in the coating.

XRD spectra of the coated specimens by concentrations of 0, 15, 20 and 25 g/l Al_2O_3 powder are shown in Fig. 3. By an increase in alumina concentration in the electrolyte to 20 g/l the relative intensity of Al_2O_3 diffraction peaks are increased. More powder concentration in the bath leads to more relative intensity of Al_2O_3, and it decreases with increasing the amount of powder in electrolyte. That shows the produced coating in concentration of 20 g/l alumina powder in the watts bath has the most amount of second phase particles compared to other specimens.

One of the most important properties of a coating is microhardness. In fig. 4, variations of Ni crystallite sizes (fig. 4a) and microhardness (fig. 4b) of the composite coatings versus concentration of Al_2O_3 particles in the baths have been demonstrated. Increasing of second phase particles in the coating results in lower grain sizes and higher microhardness. In others works [20-22] it has been shown that Ni electroplates have a columnar structure. Additions of ceramic particles such as alumina stops the columnar growth of previously nucleated Ni grains so that new Ni clusters must nucleate and Ni crystallite size becomes lower and the microhardness of the coating increases. According to fig. 4, the coating electroplated in the bath with 20 g/l alumina (which has the maximum Al_2O_3 content) has the minimum crystallite size and the maximum microhardness.

Although high microhardness is a desirable property for the composite coatings, mechanical mismatch between hard and brittle coating and soft and ductile substrate is the most important reason of low adhesion and delamination of the coatings. To solve this problem, functionally gradient composite coatings are developed, in such coatings the amount of second phase near the substrate is

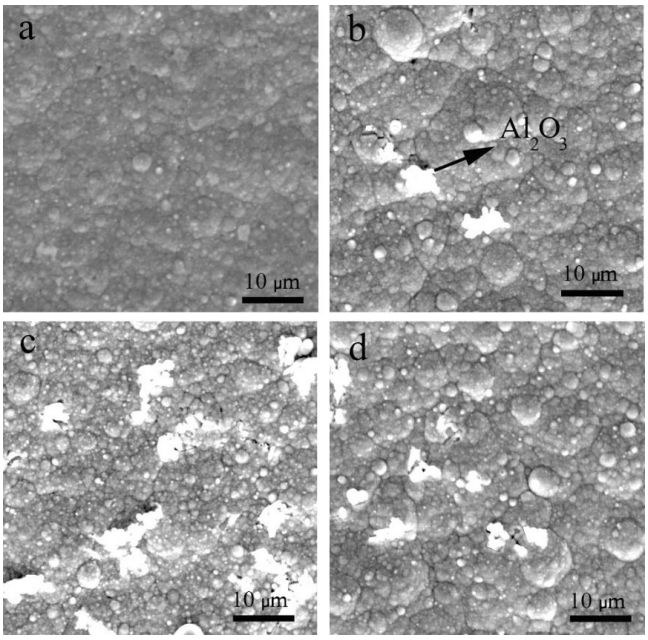

Fig. 2- SEM micrographs of the samples electroplated in the electrolytes containing alumina powder concentrations of (a) 0 g/l (pure Ni coating); (b) 15 g/l; (c) 20 g/l; (d) 25 g/l.

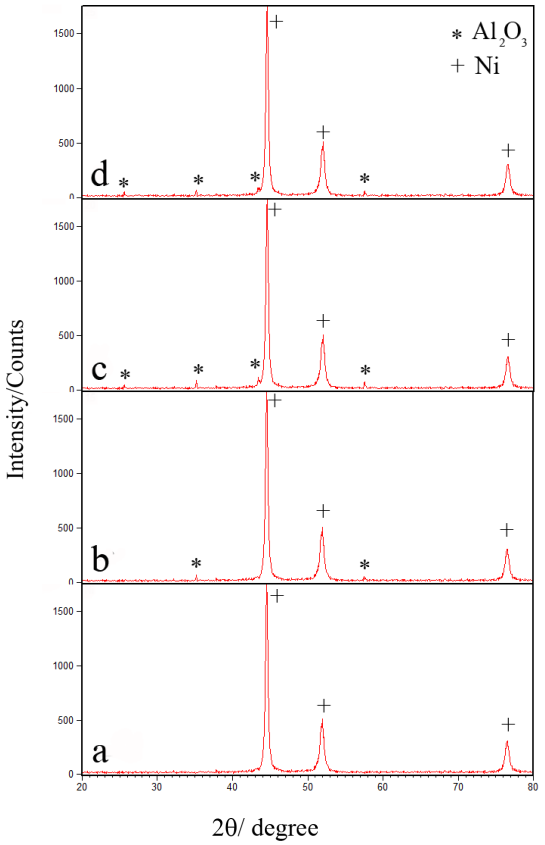

Fig. 3- XRD spectra for the samples which have been electroplated in the electrolytes containing alumina powder concentrations of (a) 0 g/l (pure Ni coating); (b) 15 g/l; (c) 20 g/l; (d) 25 g/l.

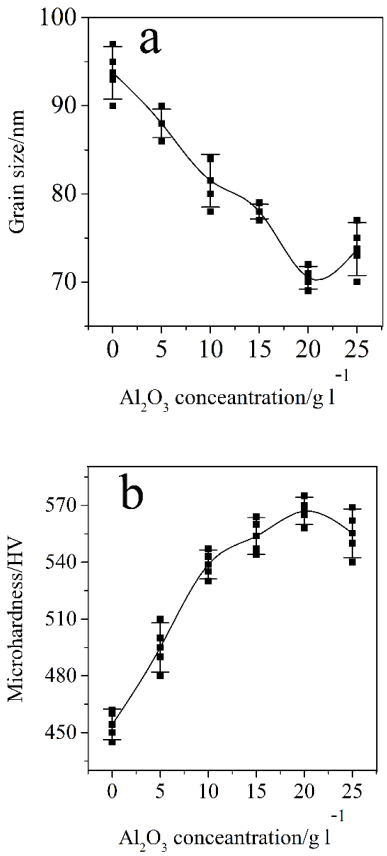

Fig. 4- The effect of concentration of particles in the bath on (a) grain size composite coatings; (b) microhardness composite coatings.

low and the microhardness of the coating and mechanical mismatch between substrate and the coating are low, but by approaching the surface, the amount of the particles increases so that a high microharness is achieved. To produce a functionally gradient composite coating, controlling of a parameters which can affect the co-electrodeposited particles content is needed. To produce Al_2O_3 content graded Ni-Al_2O_3 composite coating, the concentration of particles in watts bath was continuously increased from 0 to 20 g/l while the stirring rate of electrolyte was 200 rpm.

The EDS Mapping of the matrix (Ni) has been illustrated in Fig. 5a and Al element in FGN-A is also shown in Fig. 5b which indicates that the amount of second phase has been increased from the interface to the surface. Hence it could be stated that controlling the amounts of Al_2O_3 concentrations in the electrolyte is a reliable rout to manufacture functionally graded composite coating successfully.

Microhardness values of FGN-A cross-section has been plotted in Fig. 6. As it's shown; the microhardness of FGN-A ascended from 460 HV near the substrate/coating interface and finally reached 570 HV at the coating surface. The growing process in microhardness is due to simultaneous effects of gradually increase in amounts of Al_2O_3 particles, deposited in the coating, and decrease in grain size of the Ni matrix from interface of substrate/coating to the surface of the FGN-A. According to the relationship between microhardness and Young's modulus; the equality of the microhardness of coating and substrate at the interface; might be a reason for the coherency of their Young's modulus. So; the mechanical mismatch in the interface decreases. This way, adhesion of the coating enhances and also risks of delamination and spallation decreases. Wear-resistive property of the coating also increases due to high microhardness amounts near the surface.

Figure 7 presents comprehensive SEM photos of three types of coating that has undergone wear test. Fig. 7a shows wear track for pure Ni coating. The pure Ni makes the coating more ductile that enters the plastic deformation region under loading. Lower hardness of this coating results in considerably higher amount of adhesive wear. Although, in UN-A; the coating was worn less than pure Ni coating. Addition of ceramic Al_2O_3 particles that enhances the microhardness causes higher wear resistance compared to the pure Ni coating. The wear in this composite was abrasive because of the lack of plastic region for the coating (Fig. 7b). Micro cracks produced while sliding are probably due to compression and tensile stress in

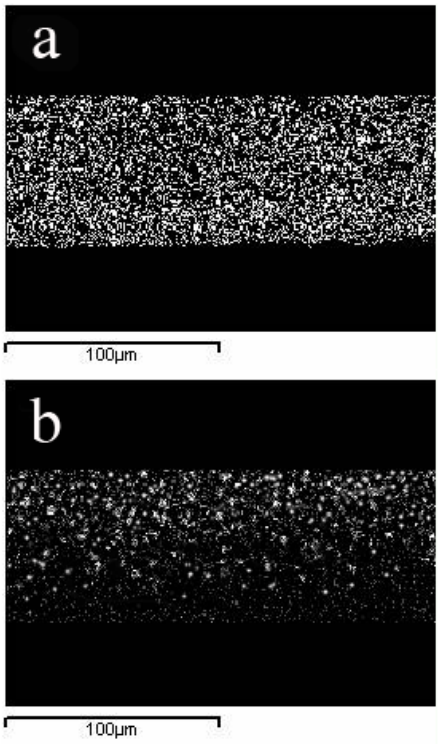

Fig. 5- (a) X-ray map of Ni and (b) X-ray map of Al in the FGN-A composite coating.

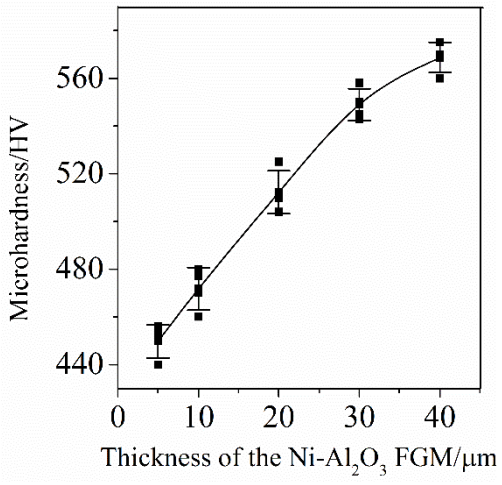

Fig. 6-Microhardness values versus thickness of the FGN-A composite coating.

surface of the coating. Cracks growing into coating can lead to coating's delamination [23, 24]. The FGN-A composite coating subdues this problem by sustaining wear test loads. The non-uniform gradient distribution of the Al_2O_3 particles results in lower stress concentration through the coating. The FGN-A composite coating wear track is demonstrated in figure 7c.

The EDS analysis of the regions that are marked by arrows in figure 7c, shows that these black areas were iron and oxygen. The Fe element exists inside the track is considerably higher than two unworn sides and is also higher than other coatings as qualitatively in figure 7c. Amounts of the element weight percent, are listed in table 2, also confirmed a quantitative measure for the iron oxide that is remained on the tribological layer. It seems that these black areas on surface coating are peeled material from steel pin that are oxidized on the wear track and create an oxide layer in connecting areas between coating and the pin. This tribological oxide layer can be a lubricant layer in connecting areas between coating and the pin, and cause a reduction in the amount of friction coefficient and also a decrease in the amount of wear rate in the coating [25].

Weighting of the coated samples and the steel pin before and after the wear test indicates that

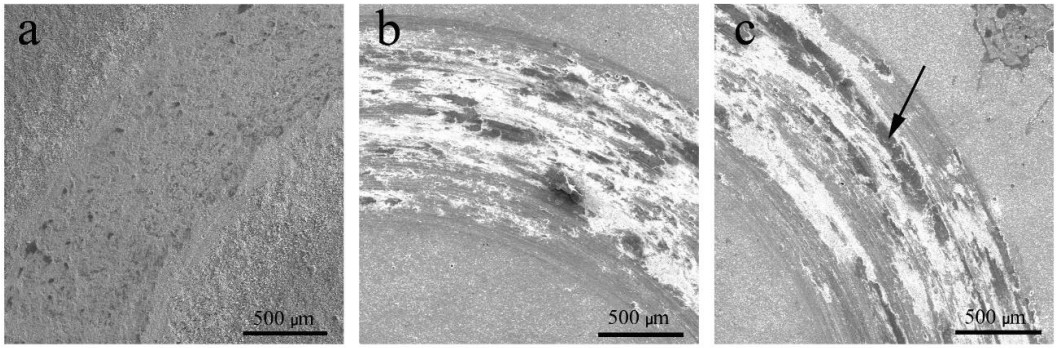

Fig. 7- The SEM worn surfaces of the coatings: (a) Ni coating, (b) UN-A composite coating and (c) FGN-A composite coating.

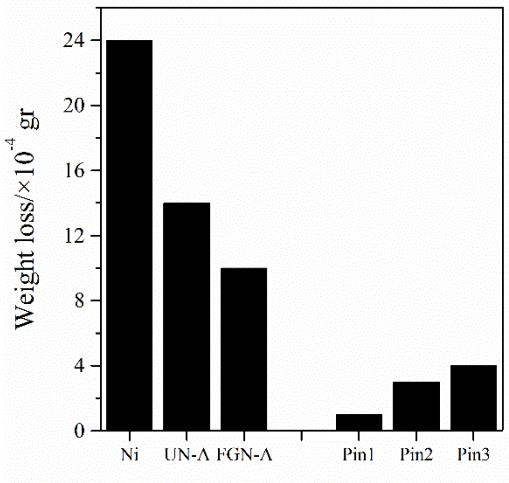

Fig. 8- Weight loss of coatings and corresponding material removal rate of the pins.

Table 2- The results of EDS analysis of the worn surface of FGN-A composite coating

Sample	Ni (wt-%)	Al (wt-%)	Fe (wt-%)	O (wt-%)
Area without tribological layer	76.70	14.46	0.11	8.73
Tribological layer	65.69	10.23	11.03	13.05

minimum weight loss belongs to the FGN-A while its test pin (pin 3 in figure 8) owned maximum weight loss. Greatest weight loss belongs to the pure Ni coating. The production of iron oxide layer on FGN-A beside low level of stress in comparison to UN-A can be a reason to lower weight loss of this coating [24, 25].

In order to investigate the adhesion of coatings each two UN-A (a-1) and FGN-A (a-2) samples were bent for 90° and the outside of the samples that are shown with an arrow in Fig. 9 were studied. Study of the surface coatings shows that cracks on the surface of UN-A composite coating (b) are more, and wider than that of FGN-A composite coating (c), that shows more adhesion of FGN-A to substrate compared to adhesion of UN-A to its substrate. This is because of bigger grain size of coating near the interface and high ductility of FGN-A than UN-A. Due to the relationship between microhardness and Young's modulus, approximately same microhardness of coating and substrate, near the interface leads to the same Young's modulus of coating and substrate so the adhesion of FGN-A composite coating compared with UN-A composite coating is increased [26]. Also gradually increase in coating's microhardness from interface coating/substrate to surface of the coating and decrease internal stress concentration in coating leads to a change in mechanical properties of FGN-A compared with UN-A [14, 27].

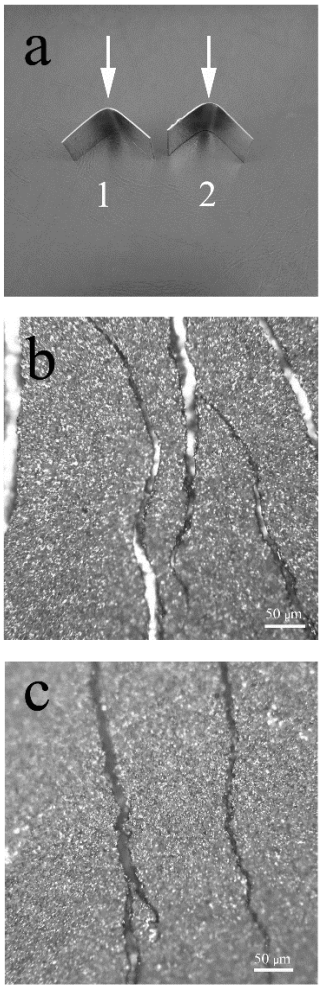

Fig. 9- Bending test results: (a) Typical samples after bending test: (a-1) substrate with the UN-A composite coating, (a-2) substrate with the FGN-A composite coating; (b) cracked UN-A after test; (c) cracked FGN-A after test.

4. Conclusions

- In this study, the FGN-A composite coating was electroplated successfully by gradually increase in concentration of Al_2O_3 from 0 to 20 g/l in the bath during electrodeposition.
- Microhardness uniformly ascended from 460 HV near the substrate/coating interface and finally reached 570 HV at the coating surface. The growing process in microhardness is due to simultaneous effects of gradually increase in amounts of Al_2O_3 particles, deposited in the coating, and decrease in grain size of the Ni matrix from interface of substrate/coating to the surface of the FGN-A composite coating.
- FGN-A composite coating had more wear resistance than UN-A composite coating. The production of iron oxide layer on FGN-A beside low level of stress in comparison to UN-A can be a reason to lower weight loss of FGN-A.
- FGN-A shows that more adhesion to substrate compared with adhesion of UN-A to its substrate. This is because of bigger grain size of coating near the interface and high ductility of FGN-A than UN-A.

References

1. Gyawali G, Tripathi K, Joshi B, Lee SW. Mechanical and tribological properties of Ni-W-TiB2 composite coatings. Journal of Alloys and Compounds. 2017;721:757-63.
2. Alizadeh M, Mirak M, Salahinejad E, Ghaffari M, Amini R, Roosta A. Structural characterization of electro-codeposited Ni–Al2O3–SiC nanocomposite coatings. Journal of Alloys and Compounds. 2014;611:161-6.
3. Arghavanian R, Ahmadi NP, Yazdani S, Bostani B. Investigations on corrosion proceeding path and EIS of Ni–ZrO2composite coating. Surface Engineering. 2012;28(7):508-12.
4. Walsh FC, Low CTJ, Bello JO. Influence of surfactants on electrodeposition of a Ni-nanoparticulate SiC composite coating. Transactions of the IMF. 2015;93(3):147-56.

5. Hefnawy A, Elkhoshkhany N, Essam A. Ni–TiN and Ni-Co-TiN composite coatings for corrosion protection: Fabrication and electrochemical characterization. Journal of Alloys and Compounds. 2018;735:600-6.
6. Calderón JA, Henao JE, Gómez MA. Erosion–corrosion resistance of Ni composite coatings with embedded SiC nanoparticles. Electrochimica Acta. 2014;124:190-8.
7. Arghavanian R, Bostani B, Parvini-Ahmadi N, Yazdani S. Field-enhanced co-electrodeposition of zirconia particles with a magnetic shell during Ni electrodeposition. Surface and Coatings Technology. 2014;258:1171-5.
8. Arghavanian R, Bostani B, Parvini-Ahmadi N. Characterisation of coelectrodeposited Ni–Al composite coating. Surface Engineering. 2014;31(3):189-93.
9. Bostani B, Arghavanian R, Parvini-Ahmadi N. Study on particle distribution, microstructure and corrosion behavior of Ni-Al composite coatings. Materials and Corrosion. 2010;63(4):323-7.
10. Jasim KM, Rawlings RD, West DRF. Metal-ceramic functionally gradient material produced by laser processing. Journal of Materials Science. 1993;28(10):2820-6.
11. Orlovskaja L, Periene N, Kurtinaitiene M, Bikulčius G. Electocomposites with SiC content modulated in layers. Surface and Coatings Technology. 1998;105(1-2):8-12.
12. Kim SK, Yoo HJ. Formation of bilayer Ni–SiC composite coatings by electrodeposition. Surface and Coatings Technology. 1998;108-109:564-9.
13. Kokini K, Choules BD. Surface thermal fracture of functionally graded ceramic coatings: Effect of architecture and materials. Composites Engineering. 1995;5(7):865-77.
14. Wang L, Gao Y, Xue Q, Liu H, Xu T. Graded composition and structure in nanocrystalline Ni–Co alloys for decreasing internal stress and improving tribological properties. Journal of Physics D: Applied Physics. 2005;38(8):1318-24.
15. Dong YS, Lin PH, Wang HX. Electroplating preparation of Ni–Al2O3 graded composite coatings using a rotating cathode. Surface and Coatings Technology. 2006;200(11):3633-6.
16. Jun L, Changsong D, Dianlong W, Xinguo H. Electroforming of nickel and partially stabilized zirconia (Ni + PSZ) gradient coating. Surface and Coatings Technology. 1997;91(1-2):131-5.
17. Ding XM, Merk N. Improvement of wear and adherence properties of composite coatings by a gradual increase in particle volume fraction. Scripta Materialia. 1997;37(5):685-90.
18. Banovic SW, Barmak K, Marder AR. Journal of Materials Science. 1999;34(13):3203-11.
19. Wang H, Yao S, Matsumura S. Electrochemical preparation and characterization of Ni/SiC gradient deposit. Journal of Materials Processing Technology. 2004;145(3):299-302.
20. Arghavanian R, Parvini-Ahmadi N. The effect of co-electrodeposited ZrO2 particles on the microstructure and corrosion resistance of Ni coatings. Journal of Solid State Electrochemistry. 2010;15(10):2199-204.
21. Arghavanian R, Parvini Ahmadi N. Electrodeposition of Ni–ZrO2composite coatings and evaluation of particle distribution and corrosion resistance. Surface Engineering. 2011;27(9):649-54.
22. Arghavanian R, Parvini Ahmadi N, Yazdani S, Bostani B. Fabrication and characterisation of nickel coated Ni-NCZ (nickel coated ZrO2) composite coating. Surface Engineering. 2012;28(7):503-7.
23. Tjong SC, Lau KC. Tribological behaviour of SiC particle-reinforced copper matrix composites. Materials Letters. 2000;43(5-6):274-80.
24. Lari Baghal SM, Heydarzadeh Sohi M, Amadeh A. A functionally gradient nano-Ni–Co/SiC composite coating on aluminum and its tribological properties. Surface and Coatings Technology. 2012;206(19-20):4032-9.
25. Hou KH, Ger MD, Wang LM, Ke ST. The wear behaviour of electro-codeposited Ni–SiC composites. Wear. 2002;253(9-10):994-1003.
26. Bostani B, Arghavanian R, Parvini Ahmadi N, Yazdani S. Fabrication and properties evaluation of functionally graded Ni-NCZ composite coating. Surface and Coatings Technology. 2017;328:276-82.
27. Hadian SE, Gabe DR. Residual stresses in electrodeposits of nickel and nickel–iron alloys. Surface and Coatings Technology. 1999;122(2-3):118-35.